PROCEEDINGS OF SCIENCE

# Measurements of four-lepton production in pp collisions at $\sqrt{s} = 8$ TeV with the ATLAS detector

**Nicola Orlando on behalf of the ATLAS Collaboration***
*Aristotle University of Thessaloniki*
*E-mail:* nicola.orlando@cern.ch

A measurement of four-lepton production in proton-proton collisions at 8 TeV with the ATLAS experiment at the Large Hadron Collider, is presented. The analysis considers four-lepton production modes in the invariant mass range between 80 GeV and 1 TeV. The total and the fiducial differential cross section measurements are extracted from each of the investigated decay channels and from their combination. The combined four-lepton fiducial cross section is also measured as a function of the four-lepton invariant mass and transverse momentum. The signal-strength of four-lepton production induced by gluon-fusion for invariant mass larger than 180 GeV is presented. The data are found to agree with the theoretical predictions confirming the validity of the Standard Model with its scalar sector in a wide kinematic regime.

*XXVII International Symposium on Lepton Photon Interactions at High Energies*
*17-22 August 2015*
*Ljubljana, Slovenia*

*Speaker.





PoS(LeptonPhoton2015)085

## 1. Introduction

The study of four-lepton ($4\ell$) production with ATLAS [1] at the Large Hadron Collider (LHC) provides a clean experimental enviorment for investigating the properties of the Higgs boson [2], searching for exotic particles [3], and for tests of the Standard Model (SM) gauge symmetry [4].

This paper presents a summary of the measurement of the the four-lepton ($4\ell$, where $\ell = e$ or $\mu$) production in proton-proton collisions at 8 TeV with the ATLAS experiment at LHC [1]. The measurement is performed in three final states: $e^+e^-e^+e^-$ ($4e$), $e^+e^-\mu^+\mu^-$ ($2e2\mu$) and $\mu^+\mu^-\mu^+\mu^-$ ($4\mu$). The analysis considers all four-lepton production modes in the invariant mass range between 80 GeV and 1 TeV: off-shell $H^*/Z^*Z^* \to 4\ell$, single resonant $Z \to 4\ell$, on-shell Higgs production $H \to 4\ell$, $ZZ^* \to 4\ell$, and on-shell diboson $ZZ \to 4\ell$. The Feynman diagrams for the most important signal processes are shown in Fig. 1.

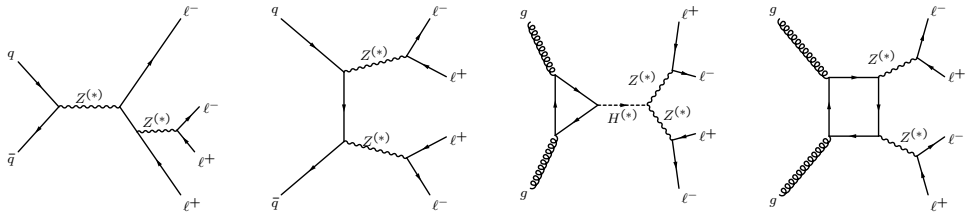

**Figure 1:** Main Feynman diagrams for the $4\ell$ signal. Taken from Ref. [1].

At low $4\ell$ invariant mass, the single resonant process $Z \to 4\ell$ provides a cross-check of the detector response to the $4\ell$ topology, relevant to the Higgs decays to four-leptons. At intermediate invariant mass, the $4\ell$ cross section measurement includes the on-shell Higgs boson and on-shell $ZZ$ processes. The high $4\ell$ invariant mass region is sensitive to beyond SM physics and it has been used for constraining the total width of the Higgs boson [5].

The ATLAS detector and its various sub-detector system are described in Ref. [6].

The $4\ell$ production cross section is measured both integrated and differentially as a function of the invariant mass ($m_{4\ell}$) and transverse momentum ($p_{\mathrm{T}}^{4\ell}$) of the $4\ell$ system. Moreover, the $4\ell$ signal strength of gluon fusion ($ggF$) production relative to its leading-order (LO) QCD estimate is determined.

## 2. Signal and Background modeling

Theoretical predictions for the $q\bar{q} \to 4\ell$ production, and on-shell Higgs-boson production via the $ggF$ and vector-boson-fusion ($VBF$) mechanisms are derived with the POWHEG-BOX [7] Monte Carlo (MC) program. The available next-to-next-to-leading order (NNLO) QCD [8] and next-to-leading order (NLO) electroweak [9] (EW) corrections are applied to the POWHEG-BOX $q\bar{q} \to 4\ell$ cross section. The cross section for on-shell Higgs-boson production is taken from Ref. [10]. The MCFM [11] generator is used to describe the non-resonant $4\ell$ signal production via gluon fusion with LO accuracy, including off-shell Higgs-boson production, continuum $ZZ$ production, and their interference. The Higgs-boson production via the $VH$ and $t\bar{t}H$ mechanisms is simulated with PYTHIA8 [12]. Off-shell $VBF$ Higgs-boson production is simulated with MADGRAPH [13].

Backgrounds for this analysis are due to $Z$+jets, $t\bar{t}$, diboson ($ZW$, $Z\gamma$ and double Drell-Yan), triboson $VVV$ ($V$=$Z$, $W$), $VH$ ($H \to VV$), and $Z$+top ($Zt\bar{t}$ and $Zt$) processes. The $Z$+jets production is simulated by using both SHERPA [14] and ALPGEN [15]. The $Z\gamma$ process is simulated with SHERPA. The $t\bar{t}$ background is modeled by POWHEG-BOX. Background events from $ZH$ production, where $Z \to \ell\ell$ and $H \to VV$ ($VV = WW$ or $ZZ$ with two leptons and two neutrinos or two leptons and two jets in the final state), are simulated with PYTHIA8. $ZW$ and $tZ$ processes are simulated with SHERPA and MADGRAPH, respectively. Backgrounds from $VVV$ and $t\bar{t}Z$ are modelled with MADGRAPH. Finally, the double-Drell-Yan $ZZ$ production is modelled with PYTHIA8.

The POWHEG-BOX and MCFM generators are interfaced to PYTHIA8 for parton shower and underlying event simulation, while MADGRAPH is interfaced to PYTHIA6 [16]. The ALPGEN generator is interfaced to HERWIG [17] for the parton shower and to JIMMY [18] for the underlying event simulation. SHERPA uses built-in models for both the parton shower and underlying-event.

## 3. Event selection and background estimation

Electron candidates are reconstructed from a combination of clusters of energy deposits in the electromagnetic calorimeter matched to tracks in the Inner Detector (ID). They are required to have $p_{\mathrm{T}} > 7$ GeV and $|\eta| < 2.47$[1]. Candidate electrons must satisfy a "loose" set of identification criteria based on a likelihood discriminant [19].

The muon identification is performed according to several criteria based on the information from the ID, the Muon Spectrometer, and the calorimeter [20]. All muon candidates are required to have $p_{\mathrm{T}} > 6$ GeV. In order to reject electrons and muons from hadron decays, only isolated leptons are selected; the isolation cuts are based on ID and calorimeter requirements.

Candidate quadruplets are formed by selecting two opposite-sign, same-flavour lepton pairs ($\ell^+\ell^-$). The two leading-$p_{\mathrm{T}}$ leptons of the quadruplet must have $p_{\mathrm{T}} > 20$ and 15 GeV, respectively, while the third lepton must have $p_{\mathrm{T}} > 10$ (8) GeV if it is an electron (muon). The four leptons of a quadruplet are required to be separated from each other by $\Delta R > 0.1$ (0.2) for same (different) flavour. All the selected $4\ell$ events must have $80 < m_{4\ell} < 1\,000$ GeV.

For each channel, the lepton pair with the mass closest to the $Z$-boson mass is selected as the leading dilepton pair ($Z_1$) and its invariant mass, $m_{12}$, is required to be between 50 and 120 GeV. The sub-leading $\ell^+\ell^-$ pair ($Z_2$) with the largest invariant mass, $m_{34}$, among the remaining possible pairs, is selected in the invariant mass range $12 < m_{34} < 120$ GeV. In the $4e$ and $4\mu$ channels all possible $\ell^+\ell^-$ pairs are required to have $m_{\ell^+\ell^-} > 5$ GeV to reject events containing $J/\psi \to \ell^+\ell^-$ decays.

The dominant backgrounds for this analysis are due to $Z$+jets and $t\bar{t}$ processes where jets are misidentified as leptons; they are estimated from data. A simultaneous fit is performed to three mutually exclusive control regions enriched in $Z$+jets and $t\bar{t}$ backgrounds; the method uses a profile likelihood approach where the input template shapes for $Z+$jets and $t\bar{t}$ are obtained from

[1] ATLAS uses a right-handed coordinate system with its origin at the nominal interaction point (IP) in the centre of the detector and the z-axis along the beam pipe. The x-axis points from the IP to the centre of the LHC ring, and the y-axis points upward. Cylindrical coordinates ($r$,$\varphi$) are used in the transverse plane, $\varphi$ being the azimuthal angle around the beam pipe. The pseudorapidity is defined in terms of the polar angle $\theta$ as $\eta = -\ln[\tan(\theta/2)]$. Transverse momentum and energy are defined as $p_{\mathrm{T}} = p\sin\theta$ and $E_{\mathrm{T}} = E\sin\theta$, respectively.

simulation. The fitted yields in the control regions are extrapolated to the signal region using efficiencies obtained from simulation. The contributions from all other backgrounds are estimated from simulation.

## 4. Results

A total of 476 events are observed with a background expectation of $26.2 \pm 3.6$ events.

The cross sections, both fiducial and total, are extracted from the number of observed events by means of a profile likelihood fit, as explained in Ref. [1]. The combination of the leptonic channels is performed in an extended common phase space defined by $80 < m_{4\ell} < 1\,000$ GeV, $m_{\ell^+\ell^-} > 4$ GeV, $p_{\mathrm{T}}^{Z_{1,2}} > 2$ GeV, four leptons each with $p_{\mathrm{T}} > 5$ GeV and $|\eta| < 2.8$. The measured cross section in the common extended phase space is $\sigma^{ext} = 73 \pm 4$ (stat.) $\pm 4$ (syst.) $\pm 2$ (lumi.) fb, in good agreement with the SM prediction $\sigma^{ext_{th}} = 65 \pm 4$ fb.

The measurement of the differential cross section as a function of $m_{4\ell}$ and $p_{\mathrm{T}}^{4\ell}$ is performed in the fiducial phase space defined in Ref. [1] using a regularised bayesian unfolding [21].

The cross section in the extended phase space, is shown in Fig. 2 (a) separately for each channel and for their combination; the distributions, unfolded for detector effects, are shown in Fig. 2 (b,c) and compared to the SM theory predictions. The data points shown in the figures are the measurements with combined statistical and systematic uncertainties. The uncertainties on the cross section measurements are dominated by the statistical uncertainties of the data. The main systematic uncertainties are due to lepton reconstruction ($\sim$ 2–5 %) and theoretical uncertainties on the $4\ell$ modeling [1] (up to $\sim$ 5%).

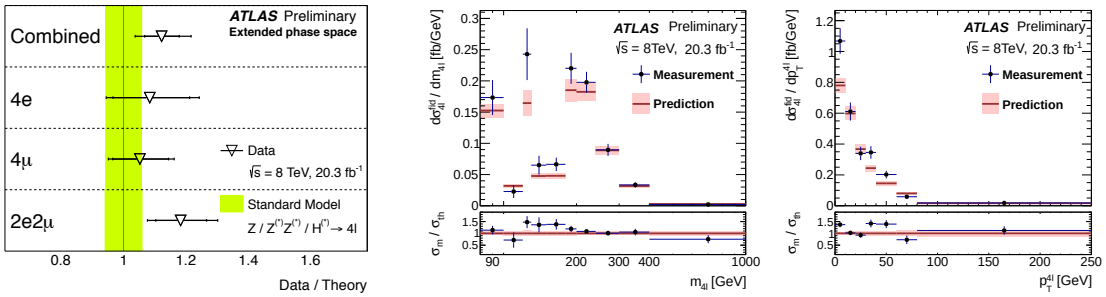


(a) (b) (c)

**Figure 2:** Cross section in the extended phase space (a), and differential cross section in the fiducial phase space as a function of $m(4\ell)$ (b) and $p_{\mathrm{T}}^{4\ell}$ (c). Taken from Ref. [1].

The signal-strength extraction of the non-resonant $gg \to 4\ell$ production is performed in the high-mass region, $m_{4\ell} > 180$ GeV, where the production mode is dominated by the continuum $gg \to ZZ$ process through a quark-box diagram intermediate state. The contribution of $qq \to ZZ$ is subtracted from data using theory predictions obtained at NNLO in QCD and corrected for NLO EW effects. The $m_{4\ell}$ spectrum is chosen as the discriminant to extract the $gg$ signal strength with respect to the LO $gg$ prediction: $\mu_{gg} = \sigma(\mathrm{data})/\sigma(\mathrm{LO})$; $\mu_{gg}$ is extracted from a likelihood fit. The fit result is $\mu_{gg} = 2.4 \pm 1.0(\mathrm{stat.}) \pm 0.5(\mathrm{syst.}) \pm 0.8(\mathrm{theory})$, which corresponds to a $gg$-initiated cross section of 3.1 fb with the same relative uncertainties as $\mu_{gg}$ itself in the fiducial phase space.

The largest uncertainty is statistical. The theoretical uncertainty is mainly due to the normalisation uncertainty of the $q\bar{q} \to ZZ$ process.

## 5. Summary

The measurement of four-lepton production in proton-proton collisions at $\sqrt{s} = 8$ TeV is presented using data corresponding to an integrated luminosity of 20.3 fb$^{-1}$ collected with the ATLAS detector at the LHC. The $4\ell$ production cross sections are measured in both the fiducial and extended phase spaces. The measured cross section in the extended phase space is $\sigma^{ext} = 73 \pm 4$ (stat.) $\pm 4$ (syst.) $\pm 2$ (lumi.) fb; the corresponding SM prediction is $\sigma^{ext_{th}} = 65 \pm 4$ fb. The $4\ell$ differential cross sections are measured as a function of $m_{4\ell}$ and the $p_{\mathrm{T}}^{4\ell}$. For $m_{4\ell} > 180$ GeV, assuming the theoretical constraint on the $q\bar{q}$ production cross section calculated with perturbative NNLO QCD and NLO electroweak corrections, the signal strength of the gluon-fusion component with respect to the LO prediction is determined to be $\mu_{gg} = 2.4 \pm 1.0\ (\mathrm{stat.}) \pm 0.5\ (\mathrm{syst.}) \pm 0.8\ (\mathrm{theory})$.

## References

[1] ATLAS Collaboration, arXiv:1509.07844 [hep-ex].

[2] ATLAS Collaboration, Phys. Rev. D **91** (2015) 1, 012006 [arXiv:1408.5191 [hep-ex]].

[3] ATLAS Collaboration, arXiv:1505.07645 [hep-ex].

[4] ATLAS Collaboration, Phys. Rev. Lett. **108** (2012) 041804 [arXiv:1110.5016 [hep-ex]].

[5] ATLAS Collaboration, Eur. Phys. J. C **75** (2015) 7, 335 [arXiv:1503.01060 [hep-ex]].

[6] ATLAS Collaboration, JINST **3** (2008) S08003.

[7] S. Alioli, P. Nason, C. Oleari and E. Re, JHEP **1006** (2010) 043 [arXiv:1002.2581 [hep-ph]].

[8] F. Cascioli *et al.*, Phys. Lett. B **735** (2014) 311 [arXiv:1405.2219 [hep-ph]].

[9] A. Bierweiler, T. Kasprzik and J. H. Kuhn, JHEP **1312** (2013) 071 [arXiv:1305.5402 [hep-ph]].

[10] S. Heinemeyer *et al.* [LHC Higgs Cross Section Working Group Collaboration], doi:10.5170/CERN-2013-004 arXiv:1307.1347 [hep-ph].

[11] J. M. Campbell, R. K. Ellis and C. Williams, JHEP **1404** (2014) 060 [arXiv:1311.3589 [hep-ph]].

[12] T. Sjostrand *et al.*, Comput. Phys. Commun. **178** (2008) 852 [arXiv:0710.3820 [hep-ph]].

[13] J. Alwall *et al.*, JHEP **1407** (2014) 079 [arXiv:1405.0301 [hep-ph]].

[14] T. Gleisberg *et al.*, JHEP **0902** (2009) 007 [arXiv:0811.4622 [hep-ph]].

[15] M. L. Mangano *et al.*, JHEP **0307** (2003) 001 [hep-ph/0206293].

[16] T. Sjostrand, S. Mrenna and P. Z. Skands, JHEP **0605** (2006) 026 [hep-ph/0603175].

[17] G. Corcella *et al.* , JHEP **0101** (2001) 010 [hep-ph/0011363].

[18] J. M. Butterworth, J. R. Forshaw and M. H. Seymour, Z. Phys. C **72** (1996) 637 [hep-ph/9601371].

[19] ATLAS Collaboration, Eur. Phys. J. C **74** (2014) 7, 2941 [arXiv:1404.2240 [hep-ex]].

[20] ATLAS Collaboration, Eur. Phys. J. C **74** (2014) 11, 3130 [arXiv:1407.3935 [hep-ex]].

[21] G. D'Agostini, arXiv:1010.0632 [physics.data-an].